


ARTICLE

Viscoelastic and electrical properties of RGO reinforced phenol formaldehyde nanocomposites

Pattoorpady Krishnan Sandhya¹ | M. S. Sreekala²  | Guijun Xian³ |
Moothetty Padmanabhan^{1,4} | Nandakumar Kalarikkal⁵ | Sabu Thomas¹

¹School of Chemical Sciences, M G University, Kottayam, Kerala, India

²Post Graduate Department of Chemistry, Sree Sankara College, Kalady, Kerala, India

³Laboratory for FRP Composites and Structures (LFCS), School of Civil Engineering, Harbin Institute of Technology (HIT), Harbin, China

⁴Department of Chemistry, Amrita Vishwa Vidyapeetham, Amritapuri, Kerala, India

⁵International and Inter University Centre for Nanoscience and Nanotechnology, M.G. University, Kottayam, Kerala, India

Correspondence

M. S. Sreekala, Post Graduate Department of Chemistry, Sree Sankara College, Kalady 683574, Kerala, India.
Email: sreekalams@yahoo.co.in

Funding information

DST-FIST, Grant/Award Number: 487/DST/FIST/15-16

Abstract

Graphene oxide was reduced (RGO) by naturally abundant potato starch and incorporated in phenol formaldehyde resin (PF). The PF/RGO nanocomposites were successfully fabricated by the combination of solution processing and compression molding. Here, nanocomposites composed of 0.05 wt% to 1 wt% RGO were prepared. The incorporation of RGO into the PF matrix was significantly affecting the dynamic mechanical characteristics of the nanocomposites such as storage and loss modulus and $\tan \delta$. The degree of entanglement (N), effectiveness of filler (β_f), reinforcement efficiency factor (r), cross-link density (v_c), and adhesion factor (A) were evaluated from the modulus values. Besides, the phase behavior of the nanocomposites was analyzed with help of Cole-Cole plot. The electrical properties of the nanocomposites have been studied concerning change in filler loading and frequency. The dielectric constant (ϵ'), dielectric loss (ϵ'') and conductivity were increased with increase in wt% of filler for the entire range of frequencies (20 Hz to 30 MHz) and the results showed that the electrical conductivity of the nanocomposites can be explained by percolation theory. The Maxwell-Garnet model was employed to calculate the theoretical dielectric constant of PF/RGO nanocomposites.

KEYWORDS

dielectric properties, mechanical properties, resins, thermosets

1 | INTRODUCTION

Phenol formaldehyde PF resins are one of the most commonly used thermosetting resins and their applications cover a wide range of predominant areas including thermal insulation materials, composites, coatings, molding compounds, structural adhesives, household appliances, wiring devices, electrical systems, and so on.^[1,2] The most prominent features that enable PF resins to be utilized in a myriad applications are excellent heat and cold resistance, low cost, easiness of production, good dimensional stability, and smoke resistance.^[3,4] On the other hand, the major challenges that are associated to the utilization

of phenolic resins based research are (a) the bulky and complex molecular structure of phenolic resin which makes a challenge for the well dispersion of nanoparticles in PF resin, (b) the release of water molecules as a by-product during the curing process which leads to the formation of voids or pores in the resin consequently, a decrement in the properties of the resultant nanocomposites will be occurred and, (c) the high crosslink density of phenolic resins makes them brittle.^[5] The incorporation of nanofillers that have varying properties can be exploited for obtaining phenolic resins with superior properties. PF is well known for its electrical insulating properties and its conductivity can be

improved by reinforcing with RGO. In the case of nanocomposites with insulating polymers and very conducting nanofillers, the main challenge is to attain the improvement in electrical properties.

Graphene, a two-dimensional carbonaceous material, can be considered as a suitable candidate for reinforcing PF resin due to its excellent mechanical, thermal and electrical properties.^[6] Even though, there are several methods used for synthesizing graphene such as micro-mechanical exfoliation, chemical vapor deposition CVD, liquid phase reduction of graphene oxide and epitaxial growth the most reliable method to prepare graphene oxide GO from graphite powder is Hoffmann method.^[7] The reduction of graphene oxide resulted in the formation of RGO with significantly less number of oxygenated functional groups. There is abundance of literature that adopted the chemical approach for reducing GO represented by hydrazine, hydrobromic, hydroiodic, and hydrochloric acids.^[7] In the current study, an ecofriendly approach represented by potato starch is adopted to obtain RGO.

Several factors affect the dielectric constant of polymeric materials, which include dipole, interfacial, electronic and atomic polarization. Among these factors, the effects of electronic and atomic polarizations are occurred at higher frequencies and are instantaneous polarization components, but the interfacial polarization affects the dielectric constant. When there are polar groups present in the molecule, dipole polarization occurs and in the case of PF, the presence of polar groups leads to high dielectric constant.^[8] On considering the effect of frequency on dielectric, (a) at low frequency there is a complete orientation of molecule occurs, (b) at medium frequency there is only little time for orientation, and (c) at higher frequencies there is no time for orientation. The study of the electrical properties of nanocomposites is of great importance on considering their applications in various fields.

The stiffness and damping properties of PF/RGO nanocomposites can be studied by the dynamic mechanical analysis DMA. PF is a thermosetting resin which shows the property of electric insulation. The electrical conductivity for PF can be improved by incorporating RGO, which has high intrinsic electrical conductivity and high aspect ratio. The PF resin can be used to prepare PF/RGO composites by applying heat and during the application of heat, PF resin undergoes condensation polymerization reaction that finally leads to a highly crosslinked PF composite with RGO embedded in the matrix.

Several studies have been reported the viscoelastic behavior of PF resins obtained by DMA and discussed the effect of different weight fractions of different

nanofillers on the mechanical properties of the resulted nanocomposites. Xu et al. (2013) prepared PF/GO nanocomposites by in-situ polymerization and studied the dynamic thermomechanical performance for investigating the thermomechanical properties of the nanocomposites.^[9] The findings showed that the storage modulus of the nanocomposites was improved. 0.5 wt% and 1 wt% GO filled composites showed an improvement of (79.8 and 78.3)% increase in storage modulus compared to pure PF. From the $\tan \delta$ curve, it was observed that Tg measured by DMA shifted higher when GO was added to PF compared to the neat polymer. Wei et al. (2015) modified GO by poly (hexanedithiol) and prepared composites using PF resin by blending, rolling and compression molding.^[10] DMA results showed that the modification of GO enhanced the rigidity of the nanocomposites, which confirmed the good dispersion and interfacial interaction between the PF and modified GO. The loss factor curves of PF/GO composites were smooth and broad; an increment in Tg was obtained for the nanocomposites compared to the pure polymer. Zhou et al. (2013) prepared PF/GO nanocomposites by solution mixing followed by molding at 180°C for 1 hr in a thermo press.^[3] DMA was employed to know the effect of GO on the thermomechanical properties of PF composites. DMA results showed that for a small amount of GO (0.5 wt%), there is an improvement in the elastic modulus of phenolic resin due to the stiffening effect of GO. The presence of GO hinders the movement of the PF chain and as a result, the $\tan \delta$ of GO/PF composites is much lower than that of PF resin. There is an improvement in the heat resistance of PF by 31.4°C with the addition of GO.

The factors that affect the conductivity of polymer nanocomposites are the concentration of filler, aggregation of filler, processing methods, functionalization and aspect ratio of graphene sheets, inter-sheet junction, distribution in the matrix, wrinkles, and folds. Yuan et al. (2014) reported an efficient one-step approach to reduce and functionalize GO during the in-situ polymerization of phenol and formaldehyde.^[11] They observed that RGO sheets improved the electrical conductivity of PF nanocomposites with a percolation threshold of 0.17 vol%. Zhao et al. (2014) prepared PF/RGO nanocomposites by in-situ polymerization and found that samples with 0.1–0.5 wt% RGO showed an increase in electrical conductivity.^[12] The highest electrical conductivity was observed for 0.5 wt% RGO (1 order of magnitude higher than that of pure polymer) due to the effective network formed by the homogeneous dispersion of RGO sheets in the PF matrix. Jiyang et al. (2017) fabricated nanocomposites via solution mixing followed by cured in a vacuum oven.^[13] The synthesized hybrid nanocomposites with 4 wt% of nanofiller exhibited high electrical conductivity of 27.2 S/m.

The present study aimed at analyzing the effect of RGO on the dynamic and electrical properties of PF resin. Degree of entanglement, the effectiveness of filler, reinforcement efficiency factor and crosslink density were also determined from storage modulus values. The damping factor and adhesion factor were also analyzed and the structural changes were studied with the help of Cole–Cole plot. Here, the effect of RGO on the electrical properties of PF nanocomposites was studied. The theoretical dielectric constant of PF nanocomposites was determined by the Maxwell-Garnet equation. DC conductivity studies of PF nanocomposites with varying content of graphene derivatives were included in this work. The study of dynamic mechanical and electrical properties of PF/RGO nanocomposites is of substantial practical significance due to their unique applications in engineering components. DMA measurements give accurate information about glass transition, entanglement density, reinforcement efficiency of nanofiller and adhesion factor. The conductivity measurements give information about the effect of RGO sheets on the conductivity of the PF matrix. It is evident from the results that the improved mechanical and electrical properties of PF/RGO nanocomposites will be used for several advanced engineering applications like aerospace, construction industries, and communications.

2 | EXPERIMENTAL PART

2.1 | Materials

Graphite powder (molar mass 12.01 and particle size $<50\ \mu\text{m}$), NaNO_3 (99%), Conc. H_2SO_4 (98%), KMnO_4 (99%), hydrogen peroxide (30% in water), and ammonia (25%) were purchased from Merck, India. Starch potato (~84%) is procured from LOBA Chemie Pvt. Ltd. Phenol formaldehyde resole resin was purchased from Polyformalin (Ernakulam, Kerala).

2.2 | Preparation of the PF/RGO polymer nanocomposites

Graphene oxide was obtained by the Hummers method from graphite powder and reduced by starch potato. The samples were prepared by solution mixing method followed by compression molding. The weight of RGO was taken based on solid content of PF resin, wet with acetone and mechanically stirred for 2 hr followed by sonication for 1 hr. The sample is later compression molded at 100°C for 30 min. The detailed method of preparation and characterization of RGO and PF/RGO

nanocomposites were explained in our research article published elsewhere.^[14,15]

2.3 | Characterization of PF/RGO nanocomposites

The dynamic mechanical analysis of the prepared PF nanocomposites was performed using a Dynamic Mechanical Analyzer DMA Q800 (TA instruments Co.) in a single cantilever mode in the frequency range of 1 Hz. Rectangular samples of dimensions length 35 mm, width 5 mm and thickness less than 2 mm were used for the analysis. The samples were heated from room temperature to 180°C at a heating rate of $2^\circ\text{C}\ \text{min}^{-1}$. The dielectric properties of the samples were measured using Wayne Kerr 600B precision LCR meter with frequency ranging from 20 Hz to 30 MHz. Electrical resistivity of the prepared nanocomposites was measured using Keithley electrometer 6517B by two probe method ($70\ \text{mm} \times 70\ \text{mm} \times 2\ \text{mm}$) with a test fixture (Keithley, 8009).

3 | RESULTS AND DISCUSSIONS

3.1 | Storage modulus (E')

The viscoelastic properties and transition temperatures of the cured composites can be studied by DMA. Figure 1a illustrates the effect of RGO at various wt% on the storage modulus of PF/RGO composites. It is observed that the storage modulus decreased with an increase in temperature in all cases. Below T_g (122.72°C from DMA analysis), storage modulus value is high because the components are in close, tightly packed and in a frozen state.^[16] The polymer chains undergo deformation as a result of bending of chemical bond present in them and the mechanical strengths corresponding to them reaches the maximum at low temperature. At a particular temperature, the deformation of the polymer chain becomes maximum and a significant decrease in storage modulus is observed. At this temperature range, a phase transition from a rigid glassy state to a flexible rubbery state occurred and is observed around $50\text{--}110^\circ\text{C}$. When the temperature increases, the interactions between polymer chains lose and attain molecular mobility, resulting in a decrease in storage modulus. With the increase in temperature, the bonding between PF and RGO becomes weak and leads to a reduction in the stiffness of the material. It is interesting to note that the addition of small and higher amounts of RGO produced no significant effect on the storage modulus of the nanocomposites, but a particular weight percentage of RGO has an appreciable impact on the whole

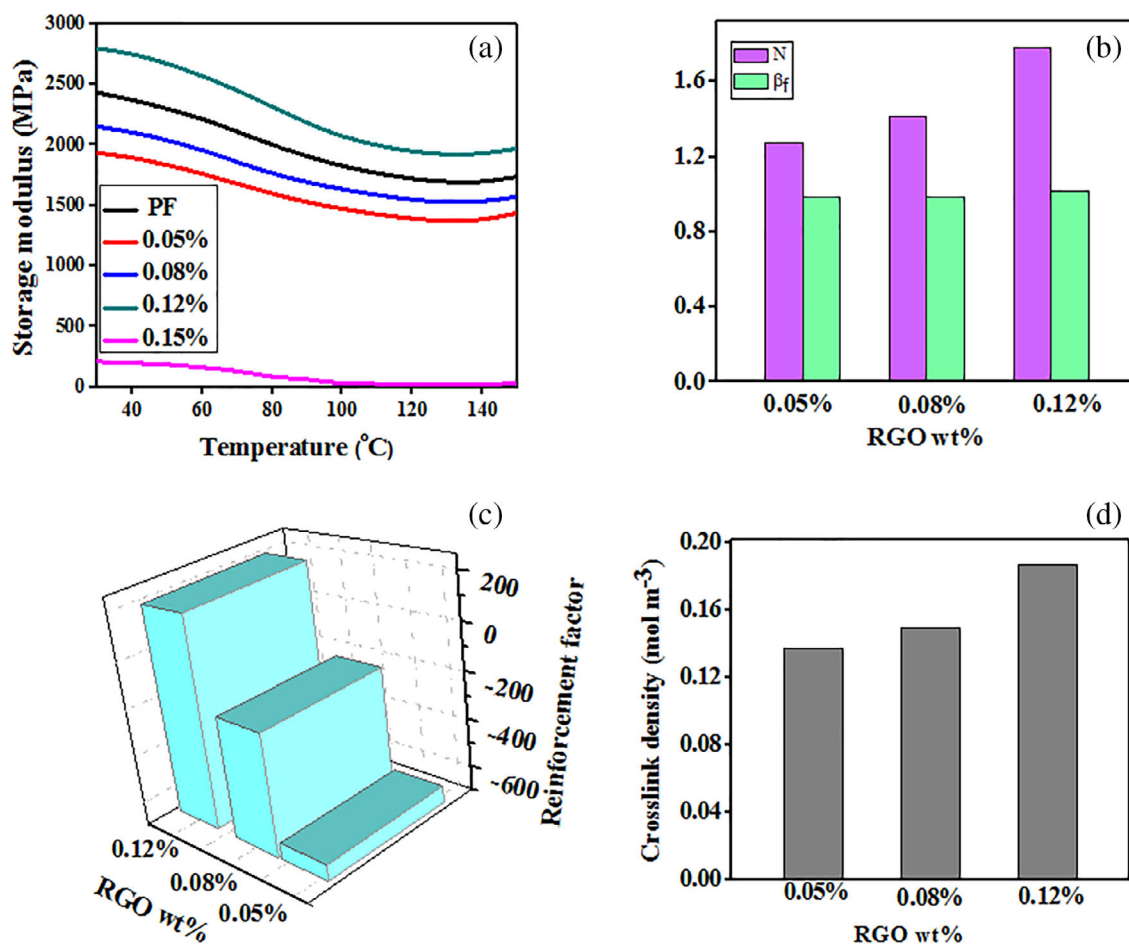


FIGURE 1 (a) Variation in storage modulus as a function of temperature, (b) degree of entanglement and effectiveness of filler, (c) reinforcement efficiency factor, and (d) crosslink density of PF/RGO nanocomposites [Color figure can be viewed at wileyonlinelibrary.com]

temperature range. In the case of nanocomposites with 0.05 wt% and 0.08 wt% shows a slight decrease in storage modulus than neat PF due to the secondary relaxation caused by side group or end group motion of polymers. Similar results were observed in polyimide/reduced graphene oxide nanocomposites.^[17] The maximum value of storage modulus is observed for 0.12 wt% RGO and it is 15% more than that of neat PF because of the strong interfacial interaction between RGO sheets and PF matrix. At this particular wt%, the RGO sheets can restrict the chain mobility of the PF matrix and increase the energy storage capacity of the PF matrix. The minimum value of storage modulus is observed for PF nanocomposites with 0.15 wt% RGO nanocomposites and is due to the aggregation of RGO sheets in the PF matrix. At higher wt% RGO, the effective interaction between the PF chains and RGO sheets becomes less and as a result, the PF chains can easily undergo molecular mobility which resulted in a decrease in storage modulus. The rubbery plateau region

observed after the glass transition region also follows the same trend.

From the value of storage modulus (E'), the degree of entanglement between polymer and filler in the polymer nanocomposites can be calculated.^[18] The degree of entanglement (N) can be calculated by using the equation

$$N = \frac{E'}{RT} \quad (1)$$

where E' is the storage modulus, R is the universal gas constant, and T is the absolute temperature. Figure 1b represents the degree of entanglement of PF/RGO nanocomposites calculated in the rubbery region at 130°C. The entanglement density with the loading of RGO sheets in the PF matrix confirms the interaction between PF and RGO sheets. The degree of entanglement of the nanocomposites showed an increasing trend with the increase in the content of RGO. Jyothi et al. (2018)

also studied the degree of entanglement of polymer nanocomposites reinforced with graphene oxide-carbon nanotube hybrid and observed an increase in the degree of entanglement with the increase in the content of nanofiller.^[19] The maximum value of N is observed for composites with 0.12 wt% RGO and is due to the good physical interaction between RGO and PF matrix.

The effectiveness of fillers on the storage moduli of the nanocomposites can be calculated from the equation

$$\beta_f = \frac{(E'_g/E'_r)_{\text{composite}}}{(E'_g/E'_r)_{\text{polymer}}} \quad (2)$$

where E'_g and E'_r are the storage modulus values of the glassy and rubbery regions respectively. Here, the values of E'_g and E'_r are considered as the storage modulus values at 30°C and 125°C, respectively. Figure 1b illustrates the values of β_f for PF/RGO nanocomposites with a varying weight percentage of RGO. The value of β_f represents the relative measurements of the modulus drop of the material with an increase in temperature when the material passes through the glass transition temperature. Smaller the value of β_f , greater will be the effectiveness of filler^[20,21] and is due to the higher degree of dispersion of filler. The maximum stress transfer between the filler and the matrix is indicated by a low β_f value because the factors such as the strength of intermolecular forces and the method by which the polymer chains are packed determine the modulus in the glassy state. From Figure 1b, a slightly high value of the effectiveness of filler is observed for neat PF indicates lower effectiveness of filler. The high value of β_f is due to the less proficient distribution of fillers in the polymer matrix.^[22] A low β_f value indicates that the effectiveness of RGO is maximum in the PF matrix because of the absence of agglomeration and restacking of RGO sheets. Similar results were also reported in the case of nanofillers such as graphene oxide and carbon nanotube reinforced polymer nanocomposites prepared by Jyoti et al. (2018, 2016) and Bagotia et al. (2019).^[19,23,24]

Apart from the values of N , the information regarding the reinforcement efficiency factor (r) can also be extracted from the storage modulus. The reinforcement efficiency factor gives an idea about the filler matrix bonding by considering the effect of fractional addition of nanofiller into the polymer matrix. The value of r is calculated using the Einstein equation.^[22]

$$E_c = E_m(1 + rV_f) \quad (3)$$

where E_c and E_m are the storage modulus of the composites and matrix respectively, r is the reinforcement

efficiency factor and V_f is the volume fraction of the filler. Figure 1c shows the plot of the reinforcement efficiency factor of composites with varying weight percentages of RGO. The value of the reinforcement efficiency factor increases with an increase in the content of RGO. The maximum value of the reinforcement efficiency factor is observed for PF nanocomposites with 0.12 wt% RGO content. The value of the reinforcement efficiency factor mainly depends upon the dispersion state of the filler, interfacial interaction between the filler and the matrix and also the concentration of the filler. From the values of the reinforcement efficiency factor, it is confirmed that the PF/RGO composites with 0.12 wt% exhibit better dispersion and interfacial interaction between the filler and matrix.

Crosslink density is an important factor that contributes to the physical properties of cured thermosets. Crosslink density represents the average molecular weight between crosslinks.^[25] From the theory of rubber elasticity, the modulus in the rubbery region is directly proportional to crosslink density. The variation of storage modulus in the rubbery region concerning RGO sheets represents the influence of RGO on the crosslink density of the PF matrix. The crosslink density of the prepared samples can be calculated using the equation^[20]

$$E_r = 3Av_cRT \quad (4)$$

where E_r represents the modulus in the rubbery region at temperature $T = T_g + 30^\circ\text{C}$ (in Kelvin), R is the universal gas constant ($8.314 \text{ Jmol}^{-1} \text{ K}^{-1}$), A is the front factor taken as unity, and v_c is the crosslink density. The values of crosslink density of the samples are listed in Figure 1d. The high value of the crosslink density is observed for composites with 0.12 wt% RGO, at this wt% of filler both interfacial interaction and crosslink density play an important role and in the case of lower filler loadings only interfacial interaction plays the major role in affecting the dynamic mechanical parameters of the samples.^[20] It is found that with an increase in wt% of RGO, the crosslink density of the nanocomposites increases. In these composites, two crosslinks such as RGO centered crosslinks and crosslinks between PF chains are formed which improved the stiffness of the material.^[26]

3.2 | Loss modulus (E'')

The loss modulus curve gives an idea about the maximum heat dissipated per cycle under deformation.^[23] The applied mechanical energy is not stored elastically and it is lost in the form of heat or molecular rearrangement.^[20] The energy dissipation or loss as heat

per unit cycle by the PF/RGO nanocomposites can be determined by loss modulus (E''). It represents the viscous behavior of the material. Figure 2 depicts the loss modulus curves of PF and PF/RGO nanocomposites. Here, only one loss modulus peak is observed for neat PF and RGO reinforced PF nanocomposites indicating the interfacial interaction between the filler and matrix and, there is no phase separation in the composites. With the increase in temperature the loss modulus increases, and it reaches a maximum value and then decreases in all cases. The maximum value indicates the maximum dissipation of mechanical energy and the decrease corresponds to the free movement of the polymer chains. The transition of PF chains from glassy to rubbery state is represented by the maximum of E'' and here, the maximum value is observed for 0.12 wt% RGO. The internal friction

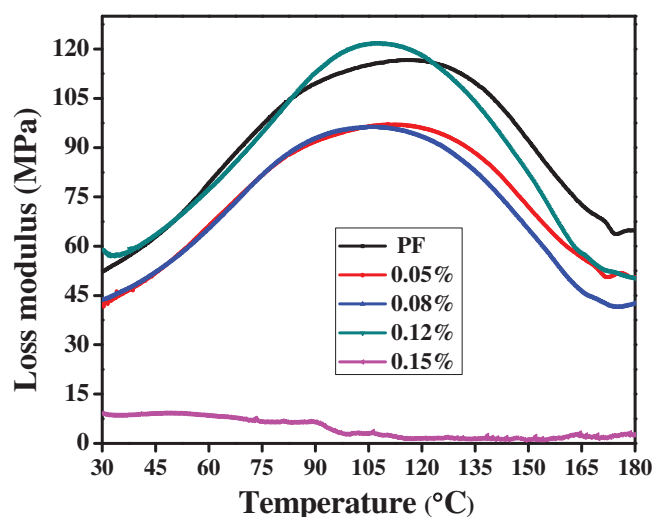


FIGURE 2 Variation of loss moduli of PF/RGO nanocomposites with temperature [Color figure can be viewed at wileyonlinelibrary.com]

between the matrix and filler as a result of different types of molecular motions, morphology and dispersion between the matrix and filler also leads to loss modulus.^[24] A variation in peak height as a result of increase in RGO content can be observed from the loss modulus curves. The maximum peak height is observed for PF nanocomposites with 0.12 wt% RGO content, which indicates higher loss modulus, higher interfacial friction, and also higher heat buildup in the composite.^[29] From the loss modulus curves, it is also observed that there is a shift in the peak position for the variation in the RGO content. Here, the peaks are shifted towards lower temperatures with an increase in the RGO content as compared to neat PF which indicates a decrease in T_g , hence the mobility of the polymer chain segments increased as a result of increased free volume with an increase in wt% of RGO.

3.3 | Damping factor (Tan delta)

The ratio of loss modulus (E'') to storage modulus (E') is called $\tan \delta$ and is a measure of damping or energy dissipation and it depends on temperature and frequency. The damping factor gives the balance between the viscous phase and elastic phase of the polymeric materials. The interface between filler and matrix, molecular weight, free volume density, and crosslink density are the factors that affect the damping factor. The T_g of PF/RGO nanocomposites were determined by the peak value of $\tan \delta$ curve and it is considered as an indicator of thermostability. Figure 3a represents the variation of $\tan \delta$ with temperature for PF and PF/RGO nanocomposites. At low temperature, the value of damping factor for all samples is small because the mobility of the chains is small. As the temperature increases, the mobility of the chains increases and the highest mobility were observed at the

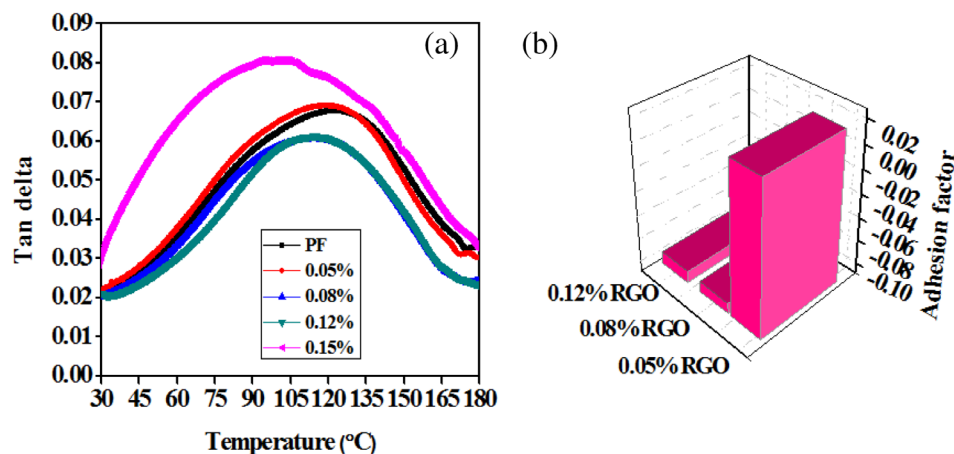


FIGURE 3 (a) Variation of tan delta with temperature and (b) adhesion factor versus concentration of RGO content [Color figure can be viewed at wileyonlinelibrary.com]

peak value of $\tan \delta$. From the figure, Tg of neat PF and its composites with 0.05 wt%, 0.08 wt%, 0.12 wt%, and 0.15 wt% of RGO is found to be 122.72°C, 118.89°C, 114.60°C, 114.38°C, and 98.56°C, respectively. There is a decrease in Tg is observed with an increase in wt% of RGO compared with neat PF. The decrease in Tg is due to the enlarged free volume between PF chains due to the reinforcement of RGO into the PF matrix. The highest mechanical damping is observed for 0.15 wt% of RGO. The high value of $\tan \delta$ indicates that the material has a high degree of non-elastic component whereas low value indicates the material has high elasticity.^[24,27] The good adhesion that exists between PF resin and RGO sheets limits the mobility of the polymer chains and decreases the values of $\tan \delta$.^[28] The low value of $\tan \delta$ is observed for composites with 0.12 wt% RGO, which shows lower damping, enhanced stiffness and good interaction between RGO and PF. The lowering of $\tan \delta$ values is an indication of improvement in the interfacial reinforcement of the nanofiller.^[29]

The value of the adhesion factor of the composites depends on the temperature and volume fraction of the filler. The values adhesion factor can be calculated from the damping behavior of the polymer matrix and composites. The adhesion factor acts as a major contributor to the performance of the composites and controls the load transfer ability of the interface between the matrix and reinforcement. Higher the value of interaction, lower will be the adhesion factor. The adhesion factor (A) can be represented as:^[23]

$$A = \frac{1}{1 - \phi_f} \frac{\tan \delta_c}{\tan \delta_p} - 1 \quad (5)$$

where ϕ_f represents the volume fraction of the filler and $\tan \delta_c$ and $\tan \delta_p$ represents the $\tan \delta$ values of composites and polymer matrix respectively. Adhesion factor values of nanocomposites with varying content of RGO are shown in Figure 3b. A decrease in the adhesion factor corresponds to an increase in the degree of interaction between the filler and matrix. At the interface region, the interaction between polymer matrix and nanoparticle reduces the molecular mobility. The decreased molecular mobility is reflected in $\tan \delta$ values and a consequent effect is observed in the values of A .^[30] The higher degree of adhesion between polymer and nanofiller is represented by a low value of the adhesion factor. The A value of the nanocomposites at higher wt% is lower than those at low wt% (0.05%). In other words, the interaction between the nanofiller and the polymer matrix is high at higher wt% of RGO. It is clearly visible from the figure that the value of the adhesion factor becomes more negative as compared to lower wt% RGO. This decrease is due to the

strong interaction between RGO sheets and PF matrix, which restricts the mobility of the polymer chains. A decrease in adhesion factor is reported in carbon nanotube reinforced polymer nanocomposites.^[30,31]

3.4 | Cole–Cole plot

The Cole–Cole plot helps to examine the structural changes that occurred in crosslinked polymers after the addition of RGO into the polymer matrix and it is valuable to measure the viscoelastic properties of polymers.^[32] Cole–Cole plot is obtained by plotting loss modulus against storage modulus and the nature of the plot is reported to be indicative of the nature of the system. In the case of homogeneous polymeric systems, the nature of the plot is a semicircle. But in the case of two phase systems, the nature of the plot is imperfect semicircular shape (elliptical path). Figure 4 shows the Cole–Cole plot for PF/RGO nanocomposites, all nanocomposites except 0.15 wt% RGO shows imperfect semicircular shape indicates the heterogeneity of the system due to strong interfacial interaction. In the case of 0.15 wt% RGO the deviation from the semicircular plot is due to the poor dispersion of nanofiller which leads to poor interfacial interaction between the PF matrix and nanofiller.

3.5 | AC conductivity

The electrical properties of the PF/RGO nanocomposites were determined by the interfacial adhesion between PF and RGO and the conductivity of the filler.^[33,34]

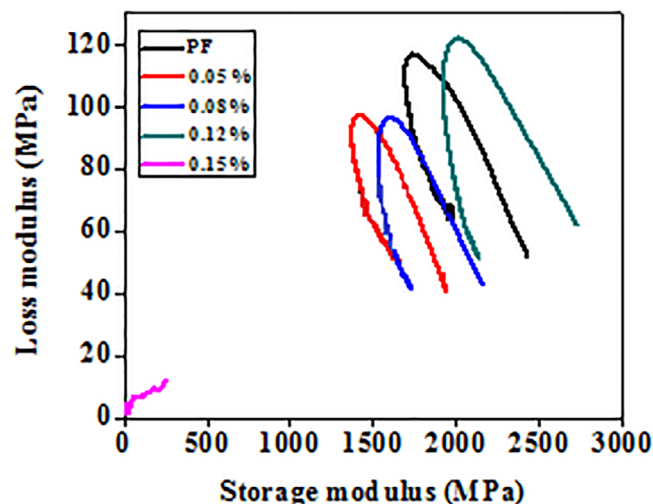


FIGURE 4 Cole–Cole plot of PF/RGO nanocomposites [Color figure can be viewed at wileyonlinelibrary.com]

Figure 5a illustrates the variation of ϵ' as a function of frequency at room temperature for PF/RGO nanocomposites. It is observed that all the samples show a gradual decrease in dielectric constant with an increase in frequency, which is in accordance with the rules of polarization relaxation.^[35] The dielectric constant of PF/RGO nanocomposites increases with an increase in wt% RGO and it is due to the incorporation of RGO into the PF matrix induces the polarization processes. The presence of sp^2 hybridized carbon atoms in the RGO sheets exhibits superior electrical properties by the delocalization of π -electrons.^[36] When an electric field is applied these π -electrons are free to move and resulted in the formation of microcapacitor and increase the dielectric constant of PF nanocomposites by the addition of RGO sheets into the PF matrix. The formation of the microcapacitor leads to the accumulation of charges on the RGO sheets when an electric field was applied.^[37] Moreover, the polarizability of PF/RGO nanocomposites increased with increasing the RGO content because of the isolation distance between the fillers gets reduced simultaneously. As a result, more charges are accumulated on the RGO sheets and thus increased the dielectric constant of PF/RGO nanocomposites.^[29]

The lowest value of dielectric constant was observed for neat PF and PF/RGO nanocomposites with 0.05 wt% RGO. In the case of other concentrations of RGO, ϵ'

increases with an increase in filler loading and decreases with an increase in frequency. The highest dielectric constant was observed for nanocomposites with 1 wt% RGO. The decrease in ϵ' with an increase in frequency was associated with the decrease of total polarization arising from the dipoles (Figure 5b). The electric dipoles present in dielectric materials tend to align the direction of the applied electric field. In the case of lower frequencies, the dipole moments can orient themselves easily in the direction of the applied electric field, which leads to a high dielectric constant. But at higher frequencies, the dipole moments become unable to follow the variations in the applied field and leads to a lower dielectric constant.^[29] The better dispersion and high aspect ratio of the RGO sheets form microcapacitors and increases the dielectric constant of PF /RGO nanocomposites.^[38]

Figure 5c represents the dielectric loss (ϵ'') of PF/RGO nanocomposites with varying RGO content. From the figure, it is observed that the dielectric loss of PF/RGO nanocomposites increases with an increase in wt% RGO. This is due to highly conductive RGO sheets which can easily form a conductive pathway in the PF matrix with the increase in wt% RGO. With increasing the filler content, PF/RGO nanocomposites become more conductive and leakage current will occur. As a result, a part of electrical energy is transformed into thermal energy.

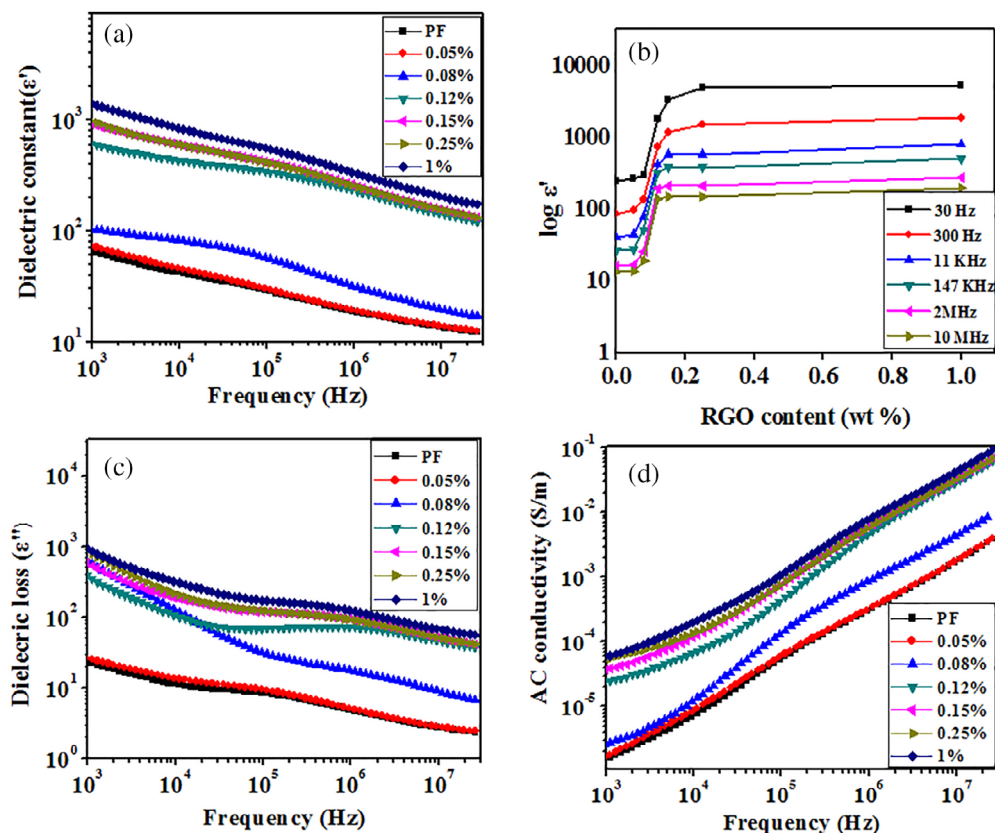


FIGURE 5 (a) Frequency dependent dielectric constant, (b) variation of dielectric constant with RGO content, (c) frequency dependent dielectric loss, and (d) AC conductivity of PF/RGO nanocomposites [Color figure can be viewed at wileyonlinelibrary.com]

The electrical conductivity of the polymer matrices can be improved with the addition of conductive nanofillers. Figure 5d represents the variation of AC conductivity of PF/RGO nanocomposites with frequency. At low frequency, the increase in AC electrical conductivity is due to the interfacial polarization.^[39] At high frequency region, the increase in AC conductivity is due to the electronic polarization. From the figure, we observe an increase in AC conductivity with increase in wt% of RGO contents.

The Maxwell-Garnet model was used to calculate the theoretical dielectric constant of PF/RGO nanocomposites according to the following equation.^[40]

$$\epsilon_c = \epsilon_m \frac{2(1-\phi)\epsilon_m + (1+2\phi)\epsilon_f}{(2+\phi)\epsilon_m + (1+\phi)\epsilon_f} \quad (6)$$

where ϵ_c , ϵ_m , and ϵ_f represents the dielectric constants of composite, matrix, and filler, respectively. ϕ represents the volume fraction of filler. Here, the value of $\epsilon_m = 13.36$ (measured value), $\epsilon_f = 18.97$ and the calculations were done at a frequency of 10 MHz. Figure 6 represents the comparison between theoretical and experimental results. The experimental and theoretical values are in close agreement at a lower volume fraction of RGO, but at a higher volume fraction of RGO the experimental values show better results than theoretical values.^[41,42] The deviations are due to various factors that affect the dielectric constant of the PF/RGO composites other than dielectric constant and volume of the filler. The size and shape of the filler, homogeneity in the distribution of the

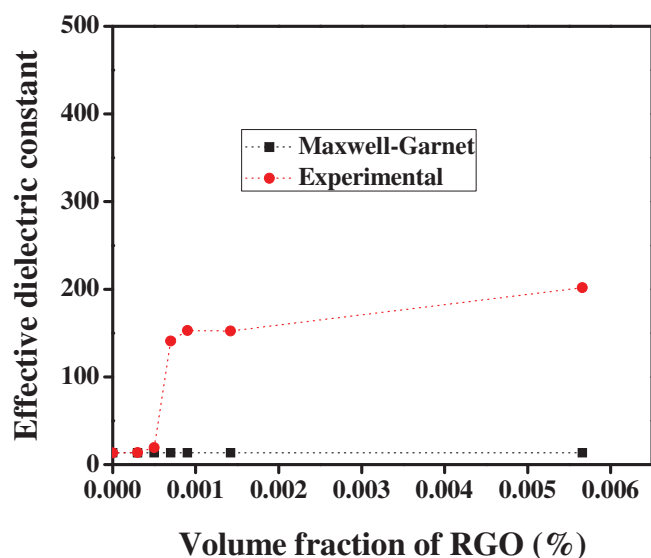


FIGURE 6 Comparison of experimental and calculated dielectric constant of PF/RGO nanocomposites [Color figure can be viewed at wileyonlinelibrary.com]

filler and the interface between filler and matrix are different factors that affect the effective dielectric constant of PF/RGO nanocomposites.^[43] The deviations exists between the calculated and theoretical values because it is difficult to consider all the above discussed factors that affect the effective dielectric constant.

3.6 | DC conductivity

Figure 7 shows the DC conductivity PF/RGO nanocomposites with different wt% of RGO. The electrical conductivity of PF/RGO nanocomposites increases with an increase in wt% of RGO, and the increase is found to be in the order of 10^{-5} S/m. The electrical conductivity of neat PF is 1.46×10^{-5} S/m. The electrical conductivity of PF/RGO nanocomposites slightly increases with an increase in wt% of RGO. When the content of RGO is very low in the PF matrix, no conductive network is formed due to the irregular distribution of RGO in the PF matrix. When the content of RGO increases, network formation of RGO in the PF matrix increases. The creation of an uninterrupted conductive channel increases the conductivity. Here, beyond 0.15 wt % RGO the electrical conductivity of the composites showed a sudden increase in conductivity. This drastic enhancement in electrical conductivity indicates the percolation threshold and it is observed between 0.15 and 0.25 wt% RGO. At percolation, a continuous conducting network is formed inside an insulating polymer matrix and only beyond the percolation there is an increase in the number of such conductive networks. There are a number of factors that affect the percolation threshold such as shape, size, aspect ratio, aggregates and the

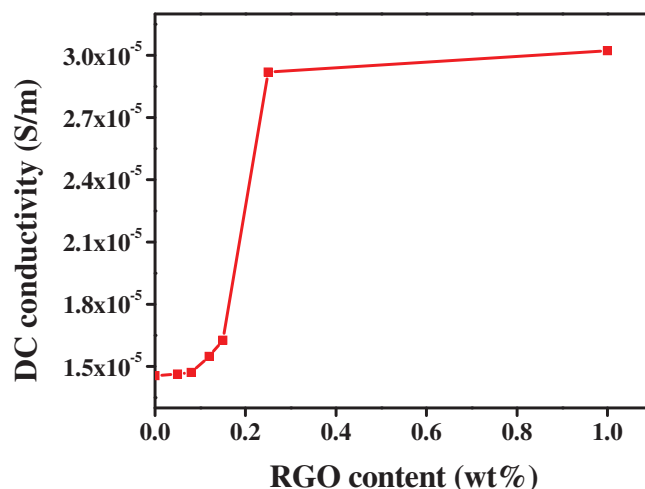


FIGURE 7 DC conductivity of PF/RGO nanocomposites [Color figure can be viewed at wileyonlinelibrary.com]

spatial distribution of filler particles in the polymer matrix, the processing methods, the adhesion and interaction between the filler and the polymer matrix.^[44,45] It is well known that if the particle size is smaller the percolation threshold will be lower. In the case of smaller particle size, the interparticle distance between RGO sheets in the matrix is small and facilitates the formation of three-dimensional networks at lower volume fractions.^[46] Moreover, the arrangement of nanoparticles on the polymer particles and the change in the morphology of the polymer matrix produced by the nanoparticles also affect the percolation threshold values.^[47] The presence of large aggregates of RGO sheets have a smaller specific surface as compared to the total specific surface area of individual nanosheets and thus they exhibit low contact resistance. On the basis of observations, it is assumed that the PF particles are surrounded by RGO nanosheets or its aggregates leads to the formation of three-dimensional conductive networks in the polymer matrix produced conductivity in the nanocomposites.

4 | CONCLUSIONS

The effect of RGO on the viscoelastic properties of PF resin was studied and found that RGO act as an effective reinforcing agent in the PF matrix. About 15% increase in storage modulus is observed for nanocomposites with 0.12% RGO than neat PF because of the strong interfacial interaction between nanofillers and PF matrix. Degree of entanglement, reinforcement efficiency factor, and crosslink density increases with an increase in wt% of nanofiller. The low value of β_f indicate maximum effectiveness of filler and is observed for 0.08 wt% nanofiller. Only one loss modulus peak is observed for PF nanocomposites indicating the interfacial interaction between the filler and matrix and no phase separation in the composites. T_g values of nanocomposites are lower than that of neat PF and it is due to the enlarged free volume between PF chains and nanofillers. The decrease in adhesion factor is observed for nanocomposites with 0.08 and 0.12 wt% nanofiller due to the good adhesion between the filler and matrix and restricts the mobility of the polymer chain. Cole–Cole plot of the PF nanocomposites showed imperfect semicircles indicating heterogeneity of the system due to the good interfacial interaction between the matrix and nanofiller.

The effect of RGO on the electrical conductivity of PF nanocomposites was evaluated. AC conductivity increases with an increase in wt% of nanofiller due to the formation of continuous conducting networks in the PF matrix. The comparison of experimental and theoretical values of effective dielectric constant was done by

Maxwell Garnet equation and results showed that the experimental values are higher than theoretical values. DC conductivity studies of PF/RGO nanocomposites shows a slight increase in conductivity in the order of 10^{-5} S/m.

ACKNOWLEDGMENTS

The authors are grateful to the financial support under DST-FIST (No. 487/DST/FIST/15-16) New Delhi to Sree Sankara College, Kalady.

ORCID

M. S. Sreekala  <https://orcid.org/0000-0002-9357-0947>

REFERENCES

- [1] G. Zhou, S. Movva, L. J. Lee, *J. Appl. Polym. Sci.* **2008**, *108*, 3720.
- [2] W. S. Solyman, H. M. Nagiub, N. A. Alian, N. O. Shaker, U. F. Kandil, *J. Radiat. Res. Appl. Sci.* **2017**, *10*, 72.
- [3] J. Zhou, Z. Yao, Y. Chen, D. Wei, Y. Wu, T. Xu, *Polym. Compos.* **2013**, *34*, 1245.
- [4] C. Yu, M. Gao, J. Feng, Y. Liu, J. Lv, H. Liu, C. Wei, *Polym. Compos.* **2017**, *38*, E351.
- [5] D. Bansal, S. Pillay, U. Vaidya, *J. Reinf. Plast. Comp.* **2013**, *32*, 955.
- [6] H. Roghani-Mamaqani, V. Haddadi-Asl, M. Mortezaei, K. Khezri, *J. Appl. Polym. Sci.* **2014**, *131*, 40273.
- [7] V. B. Mohan, K. T. Lau, D. Hui, D. Bhattacharyya, *Compos. B-Eng.* **2018**, *142*, 200.
- [8] S. Joseph, S. Thomas, *J. Appl. Polym. Sci.* **2008**, *109*, 256.
- [9] W. Xu, C. Wei, J. Lv, H. Liu, X. Huang, T. Liu, *J. Nanomater.* **2013**, *2013*, 86.
- [10] J. Wei, C. Wei, L. Su, J. Fu, J. Lv, *J. Mater. Sci. Chem. Eng.* **2015**, *3*, 56.
- [11] F. Y. Yuan, H. B. Zhang, X. Li, H. L. Ma, X. Z. Li, Z. Z. Yu, *Carbon* **2014**, *68*, 653.
- [12] X. Zhao, Y. Li, J. Wang, Z. Ouyang, J. Li, G. Wei, Z. Su, *ACS Appl. Mater. Interfaces* **2014**, *6*, 4254.
- [13] Y. Jiang, R. Sun, H. B. Zhang, P. Min, D. Yang, Z. Z. Yu, *Compos. A-Appl. Sci. Manuf.* **2017**, *94*, 104.
- [14] P. K. Sandhya, M. S. Sreekala, M. Padmanabhan, K. Jesitha, S. Thomas, *Compos. B-Eng.* **2019**, *167*, 83.
- [15] P. K. Sandhya, J. Jose, M. S. Sreekala, M. Padmanabhan, N. Kalarikkal, S. Thomas, *Ceram. Int.* **2018**, *44*, 15092.
- [16] J. Tang, H. Zhou, Y. Liang, X. Shi, X. Yang, J. Zhang, *J. Nanomater.* **2014**, *2014*, 175.
- [17] P. Liu, Z. Yao, J. Zhou, *Polym. Compos.* **2017**, *38*, 2321.
- [18] G. Moni, A. Mayeen, A. Mohan, J. J. George, S. Thomas, S. C. George, *Eur. Polym. J.* **2018**, *109*, 277.
- [19] J. Jyoti, A. S. Babal, S. Sharma, S. R. Dhakate, B. P. Singh, *J. Mater. Sci.* **2018**, *53*, 2520.
- [20] S. S. Devangamath, B. Lobo, S. P. Masti, S. Narasagoudr, *Fiber Polym.* **2018**, *19*, 1490.
- [21] P. Verma, M. Verma, A. Gupta, S. S. Chauhan, R. S. Malik, V. Choudhary, *Polym. Test.* **2016**, *55*, 1.
- [22] A. K. Pandey, R. Kumar, V. S. Kachhavah, K. K. Kar, *RSC Adv.* **2016**, *6*, 50559.

- [23] J. Jyoti, B. P. Singh, A. K. Arya, S. R. Dhakate, *RSC Adv.* **2016**, 6, 3997.
- [24] N. Bagotia, D. K. Sharma, *Polym. Test.* **2019**, 73, 425.
- [25] H. Li, E. Burts, K. Bears, Q. Ji, J. J. Lesko, D. A. Dillard, J. S. Riffle, P. M. Puckett, **2000**, 34, 1512.
- [26] B. Wu, L. Ye, Y. Liu, X. Zhao, *Polym. Int.* **2018**, 67, 330.
- [27] S. Sand Chee, M. Jawaid, *Polymers* **2019**, 11, 2012.
- [28] F. V. Ferreira, F. S. Brito, W. Franceschi, E. A. N. Simonetti, L. S. Cividanes, M. Chipara, K. Lozano, *Surf. Interfaces* **2018**, 10, 100.
- [29] T. K. Bindu Sharmila, A. B. Nair, B. T. Abraham, P. S. Beegum, E. T. Thachil, *Polymer* **2014**, 55, 3614.
- [30] J. C. Hoepfner, M. R. Loos, S. H. Pezzin, *J. Appl. Polym. Sci.* **2019**, 136, 48146.
- [31] S. S. Chauhan, B. P. Singh, R. S. Malik, P. Verma, V. Choudhary, *Polym. Compos.* **2018**, 39, 2587.
- [32] S. Manoharan, B. Suresha, G. Ramadoss, B. Bharath, *J. Mater.* **2014**, 2014, 478549.
- [33] C. Wu, X. Huang, G. Wang, X. Wu, K. Yang, S. Li, P. Jiang, *J. Mater. Chem.* **2012**, 22, 7010.
- [34] C. W. Nan, Y. Shen, J. Ma, *Annu. Rev. Mater. Res.* **2010**, 40, 131.
- [35] J. P. Peng, H. Zhang, L. C. Tang, Y. Jia, Z. Zhang, *J. Nanosci. Nanotechnol.* **2013**, 13, 964.
- [36] R. Sengupta, M. Bhattacharya, S. Bandyopadhyay, A. K. Bhowmick, *Prog. Polym. Sci.* **2011**, 36, 638.
- [37] D. Wang, X. Zhang, J. W. Zha, J. Zhao, Z. M. Dang, G. H. Hu, *Polymer* **2013**, 54, 1916.
- [38] P. Fan, L. Wang, J. Yang, F. Chen, M. Zhong, *Nanotechnology* **2012**, 23, 365702.
- [39] B. Hussien, *Eur. J. Sci. Res.* **2011**, 52, 236.
- [40] Y. Ouyang, G. Hou, L. Bai, B. Li, F. Yuan, *Compos. Sci. Technol.* **2018**, 165, 307.
- [41] H. Akhina, P. M. Arif, M. G. Nair, K. Nandakumar, S. Thomas, *Polym. Test.* **2019**, 73, 250.
- [42] L. Zhang, H. K. H. Li, M. S. Tse, O. K. Tan, E. K. Chua, C. L. Chow, C. K. Lim, K. Y. See, *Mater. Res. Bull.* **2017**, 96, 164.
- [43] G. Subodh, V. Deepu, P. Mohanan, M. T. Sebastian, *Appl. Phys. Lett.* **2009**, 95, 062903.
- [44] M. Ghislandi, E. Tkalya, A. Alekseev, C. Koning, G. de With, *Appl. Mater. Today* **2015**, 1, 88.
- [45] S. D. Gaikwad, R. K. Goyal, *Diam. Relat. Mater.* **2018**, 85, 13.
- [46] K. S. Deepa, S. Kumari Nisha, P. Parameswaran, M. T. Sebastian, J. James, *Appl. Phys. Lett.* **2009**, 94, 142902.
- [47] M. Yoonessi, J. R. Gaier, *ACS Nano* **2010**, 4, 7211.

How to cite this article: Sandhya PK, Sreekala MS, Xian G, Padmanabhan M, Kalarikkal N, Thomas S. Viscoelastic and electrical properties of RGO reinforced phenol formaldehyde nanocomposites. *J Appl Polym Sci.* 2020;e49211. <https://doi.org/10.1002/app.49211>